

A new record of Late Permian granitoid in Tra Phu-Tra Bong area, Quang Ngai (Kontum massif) and its tectonic implications

Nguyen Thi Truong GIANG^{1, 2*}

¹ Faculty of Geology, University of Science, Ho Chi Minh city, Vietnam, 227 Nguyen Van Cu street, Ward 4, District 5, Ho Chi Minh city, Vietnam.

² Vietnam National University, Ho Chi Minh city, Vietnam, 227 Nguyen Van Cu street, Ward 4, District 5, Ho Chi Minh city, Vietnam.

* Corresponding email: ngttgiang@hcmus.edu.vn

Abstract: *Tra Bong area in Quang Ngai province is located between the southern Tam Ky-Phuoc Son suture zone and the northern Kontum massif, which has recently been of broad interest to geologists. The area includes several stages of magmatic intrusions and extrusions from different origins and ages. The granitoid samples in this study are mainly granodiorite and weakly orientated medium-grained biotite granite collected in the Tra Phu, Tra Bong area. Their mineral composition is characterized by an assemblage of plagioclase, K-feldspar, quartz, hornblende, and biotite. Geochemically, they show a moderate to high SiO₂ content (63.65–69.41 wt%), Na₂O+K₂O (6.65–8.24 wt%) and indicate A/CNK ratios of < 1.1, low TiO₂, MnO, MgO and P₂O₅. The samples fall within the volcanic-arc field (volcanic-arc granites), corresponding to I-type granite. The LA-ICP-MS U-Pb zircon ages for these rocks are between 255–252 Ma that indicate the timing of magmatic emplacement during Late Permian. The geochronological results indicate that Tra Phu granitoids in the studied area are younger than previously assumed (Ordovician-Silurian). This finding confirms that they formed during the convergence of the South China and Indochina blocks as well as the Indosinian Orogeny.*

Keywords: *Kontum massif, Tam Ky-Phuoc Son suture, geochemistry, zircon U-Pb geochronology, I-type granite, Permian-Triassic.*

1. Introduction

The granitoid formations of the Tra Phu and Tra Bong areas are located in the central Vietnam (Figure 1a). They can be found all over the northern part of the Kontum massif, just south of the Tam Ky-Phuoc Son suture zone (Figure 1a). The granitoid formation is mostly composed of gabbro-diorite, diorite, granodiorite, and granite. Nguyen Van Trang (1986) classified the Tra Bong block as Ordovician-Silurian in age [1], based on a consistent relationship between granitoids and metamorphic rocks. However, no geochronological studies for these rocks and comprehensively whole-rock geochemistry have been made in this area.

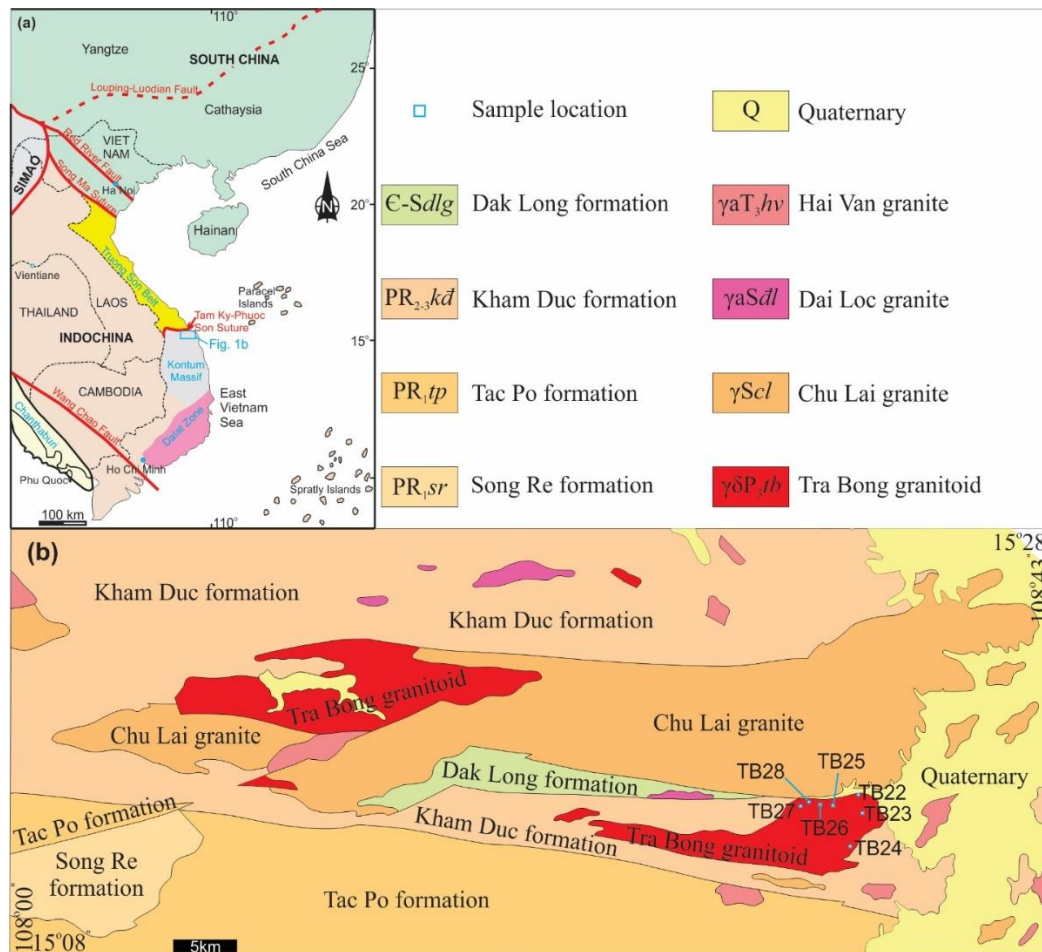


Fig. 1. (a) Location of the study area, (b) Simplified geological map of the Late Permian granitoid in the Tra Phu-Tra Bong area

The study area is the junction of many continental microplates, including Indochina, South China, and Sibumasu, undergoing many different stages of magmatic and tectonic evolution, thus making it difficult to determine the formation age. Many geologists have recently studied the magmatic rocks in the Tam Ky-Phuoc Son suture zone [2-9]. However, there are still many different discrepancies about the magmatic formations in this area [10, 11]. In this contribution, the author presents the mineral composition of granitoids from Tra Phu-Tra Bong area, with U-Pb zircon isotopic age using the LA-ICP-MS method to provide information on the petrography and formation age to contribute to explaining the origin of granitic rocks and the evolution of the continental crust in the Tra Phu, Tra Bong area; north of the Kontum massif.

2. Geological background and petrography



Fig. 2. Outcrop features of granitoid in the Tra Phu-Tra Bong area

Geologists believe that Vietnam's territory is part of the Indochina and South China blocks, with the Song Ma suture zone serving as the plate boundary [3, 6, 7]. Three major structural zones make up the Indochina block: the Dalat zone to the south, the Kontum massif to the center, and the Truong Son belt to the north. The boundary of the Kontum massif and the Truong Son belt is the Tam Ky-Phuoc Son suture zone [7, 12, 13]. The study area, located in the north of the Kontum massif (Figure 1b), includes the Song Re (PR₁), Tac Po (PR₁), and Kham Duc (PR₂₋₃) formations with the composition of biotite-hornblende gneiss, biotite gneiss, two-mica quartz schist, biotite-silimanite quartz schist, and amphibolite. To the north of the research area, Chu Lai granite appears with an enormously extensive exposure area (Figure 1b); the primary components are plagiogranite migmatite, granite migmatite, and biotite granite. Small intrusive blocks from the Dai Loc complex (gneissic two-mica granite) and the Hai Van complex (porphyritic biotite granite) can be found sporadically throughout the study area.

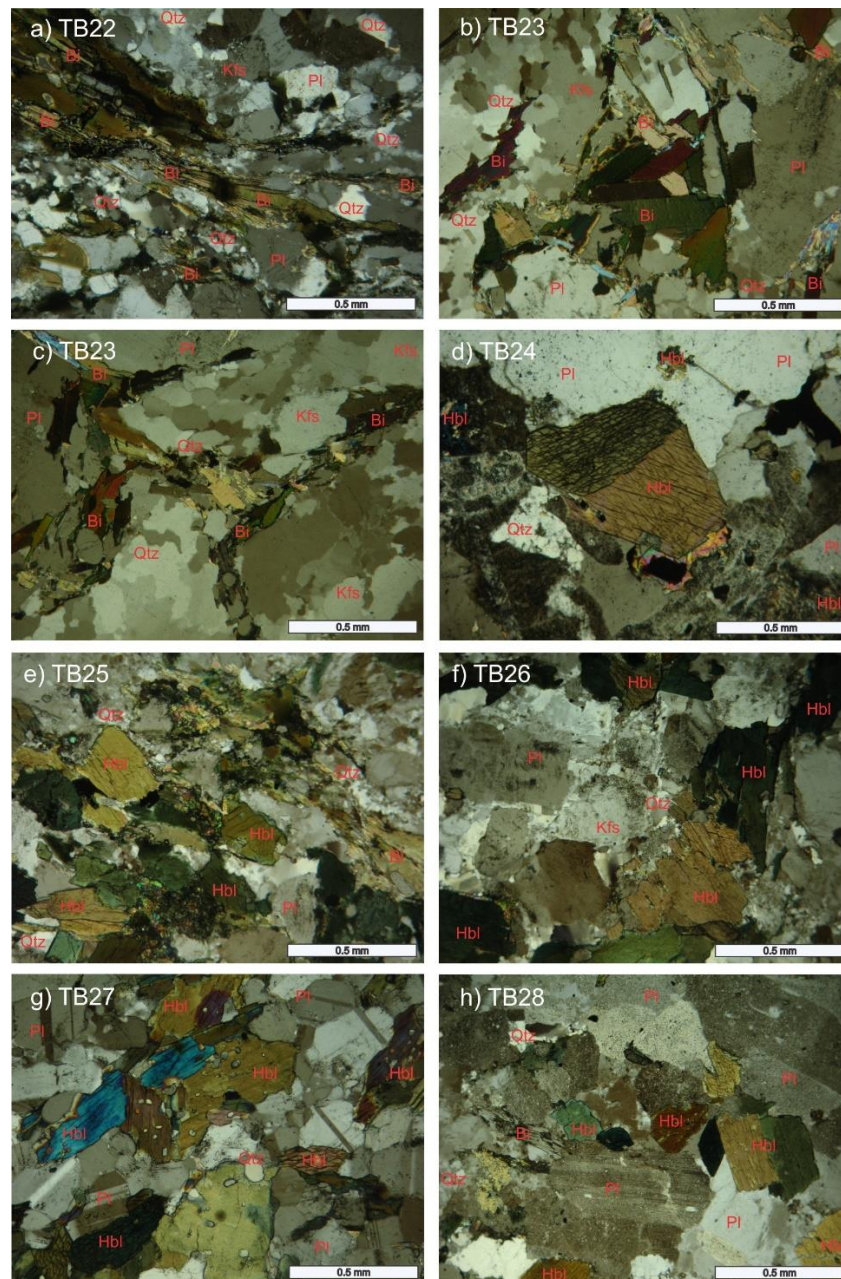


Fig. 3. Cross-polarized light photomicrographs of the Late Permian granitoid in Tra Phu-Tra Bong area. a) granite biotite, GPS: 15°15'38.8"N 108°35'23.7"E; b) and c) granite biotite, GPS: 15°14'48.2"N 108°35'25.7"E; d) granodiorite, GPS: 15°13'24.7"N 108°34'54.5"E; e) granodiorite, GPS: 15°15'09.2" N 108°34'20.8" E; f) granodiorite, GPS: 15°15'11.8"N 108°33'44.0"E; g) granodiorite, GPS: 15°15'07.2"N 108°32'53.2"E; and h) granodiorite, GPS: 15°15'18.9"N 108°33'20.9"E. Abbreviations of minerals: Pl (plagioclase), Hbl (hornblende), Bt (biotite), Qtz (quartz) and Kfs (K-feldspar).

Granitic samples obtained from Tra Phu, Tra Bong, Quang Ngai provinces, predominantly consist of granodiorite and oriented-compressed granite, which are manifested as substantial intrusive blocks that intersect the Kham Duc formation rocks. The surface is weathered in eluvial deposits with a thickness of 0.7 to 1.0 meter (Figure 2). The mineral composition consists of plagioclase (20–25%), orthoclase (15–25%), quartz (25–30%), hornblende (5–10%), and biotite (3–5%), as well as the accessory mineral sphene, which is characteristic of I-type granite. The plagioclase minerals are automorphic and range in size from medium

(0.2x0.3 mm) to big (0.4x0.9 mm). Most grain surfaces exhibit partial sericitization. The mica minerals (mostly biotite, rarely muscovite) have a moderately oriented arrangement.

3. Analytical methods

Seven granitic samples, collected in the Tra Phu and Tra Bong areas, were selected and processed for geochemical composition, and 2 granitic samples for U-Pb zircon isotope ages.

3.1. Geochemical composition analysis

Fresh rock samples were liquefied after the complete removal of heterogeneous bodies, cleaned before being grounded to a particle size < 0.074 mm. The contents of major and trace elements were determined by X-ray fluorescence (XRF) at the laboratory of the Department of Earth and Planetary Systems Sciences, Graduate School of Science, Hiroshima University, Japan. A 3 kW Rh/W dual anode tube generated X-rays and irradiated the consolidated grain samples. The analytical precision was 1σ for major elements ranging from 0.001% to 0.14 wt%, while that for trace elements was between 0.68 ppm and 2.39 ppm. The analytical results were processed using Iqpetwin software to display on the charts.

3.2. LA-ICP-MS U-Pb zircon isotopic age

Granitic samples TB27 and TB28 underwent crushing to achieve a grain size of 0.3 mm. Subsequently, they were cleaned, and the heavy and magnetic minerals were separated. The zircon grains within the non-magnetic component were isolated using the heavy solvent Bromoform (CHBr₃). Subsequently, utilizing a stereomicroscope, approximately 100 zircon grains exhibiting complete shapes were meticulously selected, while those containing inclusions and fractured zircons were excluded from the sample. The zircon grains chosen for the study were embedded in epoxy resin plates and polished down to expose their centers; following this, the samples underwent polishing, and only the euhedral grains free of defects were selected for the age analysis. Before age analysis, zircons were scanned by cathodoluminescence (CL) using a JEOL JXA8900RL electron microprobe at the Institute of Geophysics and Geology, Chinese Academy of Sciences. CL imaging took place at 15 kV and 20 nA conditions. In order to describe each grain's size, growth morphology and internal structure, typical CL pictures were acquired. These images served as a guide for our analytical spot selection process for the U-Pb dating. The isotopic composition of U-Pb was examined using the LA-ICP-MS at the Institute of Geophysics and Geology, Chinese Academy of Sciences. The isotope ratios of the samples were analyzed and dated utilizing Glitter software (Ver. 4.0, Macquarie University) and Isoplot (Ver. 2.49) to finalize the Concordia age diagram.

4. Analyze results

4.1. Geochemistry

The results of the major elements in seven representative granitic samples from the Tra Phu and Tra Bong areas (Table 1) indicate that these rocks exhibit a high SiO₂ content with relatively narrow variations ranging from 63.65 to 69.41 wt%. The TiO₂ content across all samples remains below 1.00 wt% (0.43–0.74 wt%), while the Al₂O₃ content is notably high, ranging from 14.97 to 16.12 wt%. Additionally, the total alkali content (Na₂O+K₂O) is high, falling between 6.65 and 8.24 wt%, and the K₂O/Na₂O ratio varies from 0.40 to 0.94. The aluminum saturation index ASI [(Al₂O₃)/(CaO+Na₂O+K₂O)] is high, with all values > 1.00 (i.e. 1.33 to 1.68). The MnO is 0.05–0.07 wt% and P₂O₅ is 0.15–0.35 wt%, which are notably low.

Tab. 1. Whole-rock geochemistry of the Tra Bong granite

Sample	TB22	TB23	TB24	TB25	TB26	TB27	TB28
Lithology	Biotite granite	Biotite granite	Granodiorite	Granodiorite	Granodiorite	Granodiorite	Granodiorite
Latitude	15°15'38.8"N	15°14'48.2"N	15°13'24.7"N	15°15'09.2"N	15°15'11.8"N	15°15'07.2"N	15°15'18.9"N
Longitude	108°35'23.7"E	108°35'25.7"E	108°34'54.5"E	108°34'20.8"E	108°33'44.0"E	108°32'53.2"E	108°33'20.9"E
SiO ₂ (wt%)	69.41	68.44	68.75	65.61	65.36	63.83	63.65
TiO ₂	0.44	0.44	0.43	0.66	0.62	0.74	0.70
Al ₂ O ₃	15.54	16.12	16.01	15.34	14.97	15.20	15.76

Fe₂O₃^t	2.80	2.83	2.78	3.49	3.74	4.27	4.10
MnO	0.05	0.05	0.05	0.05	0.06	0.07	0.07
MgO	1.11	1.18	1.17	1.95	2.27	2.93	2.94
CaO	2.89	2.82	2.60	3.28	3.37	3.79	4.47
Na₂O	4.59	4.84	4.97	4.32	4.04	4.40	4.66
K₂O	2.06	2.20	1.98	3.92	3.81	3.24	2.13
P₂O₅	0.15	0.18	0.21	0.30	0.30	0.34	0.35
LOI	0.95	0.92	1.06	1.08	1.45	1.22	1.18
Total	99.05	99.08	98.94	98.92	98.55	98.78	98.82
A/CNK	1.03	1.04	1.06	0.88	0.88	0.86	0.87
A/NK	1.59	1.56	1.55	1.35	1.39	1.41	1.58
Fe*	0.69	0.68	0.68	0.62	0.60	0.57	0.56
Mg#	0.44	0.45	0.45	0.53	0.55	0.58	0.59
Sc (ppm)	5.01	5.84	3.22	5.76	7.25	8.09	10.14
V	45.82	46.79	44.86	64.61	69.30	77.02	80.79
Cr	16.07	16.09	18.14	51.14	64.16	103.08	99.20
Co	6.46	5.31	4.61	8.54	10.15	12.79	12.69
Ni	7.03	7.19	7.26	26.46	35.23	53.65	46.55
Cu	6.56	8.71	8.07	13.74	30.98	24.30	14.50
Zn	63.05	55.33	39.23	69.64	70.41	78.49	72.26
Ga	20.62	20.61	20.12	22.31	19.74	19.65	21.69
Rb	98.79	106.03	101.31	116.83	110.91	99.43	55.18
Sr	499.86	528.03	512.90	1135.98	1125.26	1187.14	1613.50
Zr	179.96	164.67	146.83	192.58	179.73	188.83	163.20
Nb	16.07	13.51	14.47	9.31	10.09	9.56	8.20
Cs	5.45	6.97	4.08	8.15	8.78	6.67	3.19
Ba	538.58	604.69	562.96	944.00	945.76	752.08	676.55
Hf	6.11	7.02	5.59	12.05	12.00	14.40	15.88
Pb	22.28	21.41	20.70	23.66	24.17	18.60	18.84
Th	21.63	16.29	12.34	18.81	25.56	13.29	11.94
U	5.87	10.84	2.71	3.01	4.37	0.72	0.60
La	32.86	27.82	34.47	47.24	111.24	41.31	50.56
Ce	61.39	59.91	61.32	95.35	164.22	85.47	110.02
Nd	24.08	23.88	22.21	43.47	57.26	38.21	49.81
Yb	0.36	1.34	0.48	2.06	0.64	0.23	0.03
Y	15.04	10.13	6.37	12.02	15.26	12.20	16.19
10000Ga/Al	2.51	2.42	2.37	2.75	2.49	2.44	2.60
T Zircon	790.04	781.28	774.28	770.27	764.68	761.33	750.14
∑REE	117.97	112.95	118.48	188.12	333.36	164.76	210.36
Q (CIPW)	36.16	36.57	37.61	20.02	34.02	27.46	23.24
C	3.05	3.65	3.35	2.98	3.51	0.37	1.16
Or	25.70	23.92	27.99	24.89	28.61	25.77	28.57
Ab	24.19	23.75	25.44	39.79	28.61	35.17	42.70

An	4.32	4.39	1.66	0.65	1.38	8.04	1.66
Hy(MS)	1.73	1.57	0.77	2.68	0.74	1.56	1.25
Hy(FS)	3.51	4.86	2.17	7.33	2.04	0.47	0.78
Mt	0.36	0.47	0.22	0.69	0.20	0.08	0.08
Il	0.54	0.37	0.25	0.29	0.23	0.55	0.15
Ap	0.43	0.45	0.54	0.69	0.66	0.52	0.42

A/CNK value: molar $Al_2O_3/(CaO + Na_2O + K_2O)$; A/NK value: molar $Al_2O_3/(Na_2O + K_2O)$; T Zircon: the temperature conditions under which the zircon formed; Q: SiO_2 ; C: Al_2O_3 ; Or: $K_2O.Al_2O_3.6SiO_2$; Ab: $Na_2O.Al_2O_3.6SiO_2$; An: $CaO.Al_2O_3.2SiO_2$; Hy(MS): $MgO.2SiO_2$; Hy(FS): $FeO.2SiO_2$; Mt: $FeO.Fe_2O_3$; Il: $FeO.TiO_2$; Ap: $9CaO.3P_2O_5.CaF_2$.

The calculation of CIPW-rated minerals (Table 1) indicates the following percentages of quartz (20.02–37.61%), orthoclase (23.92–28.61%), albite (23.75–42.70%), anorthite (0.65–8.04%), ilmenite (0.15–0.55%), and magnetite (0.08–0.69%). The standard corundum index © for the majority of samples is high (> 1.00) with the maximum recorded at 3.65; however, sample TB27 falls below 1.00, registering at 0.37. The results of the CIPW calculation align with the mineral composition observed in thin-section petrographic samples.

The correlation between SiO_2 and (Na_2O+K_2O) [14], along with the Ab-An-Or rock-classification diagram according to Baker (1979) (Figure 4a, e), indicates that the majority of the samples plot within the granodiorite and granite field. The chart categorizing granite based on alkaline characteristics indicates that the analyzed samples fall within the calc-alkaline series, specifically medium-high alkaline, and are classified as Na-K alkaline ($K_2O/Na_2O < 1$). (Figure 4c, f). The correlation chart illustrating the aluminum saturation index $Al_2O_3/(CaO+Na_2O+K_2O)$ and $Al_2O_3/(Na_2O+K_2O)$ indicates that the granitic samples from the Tra Phu and Tra Bong area are I-type granite, demonstrating metaluminum saturation (Figure 4b). The correlation chart illustrating the content of K_2O and Na_2O indicates that these magma formations align with I-type granite (Figure 4d). The geotectonic classification after Pearce (1984), used to identify tectonic environments, suggested the samples were mostly plotted in the volcanic arc granite (VAG) (Figure 5) which is related to the subduction zone.

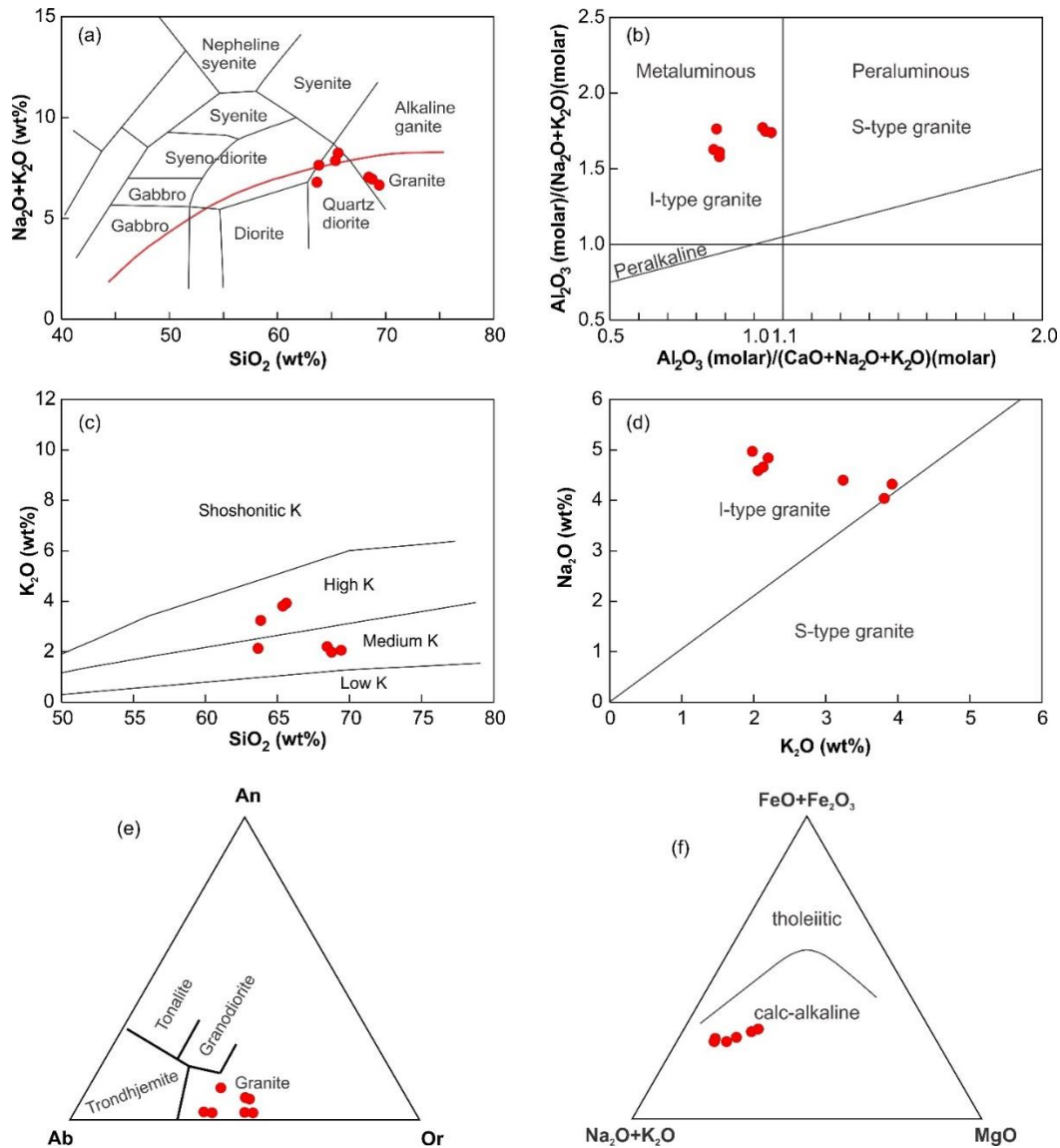


Fig. 4. Classification diagram of the Late Permian granitoid in Tra Phu-Tra Bong area. (a) TAS diagram [14]; (b) A/CNK vs A/NK diagram [16]; (c) K_2O vs SiO_2 diagram [17]; (d) Alkali concentrations discrimination diagram (K_2O - Na_2O in wt%); (e) An-Ab-Or CIPW-normative ternary diagram [18] and f) AFM diagram [19].

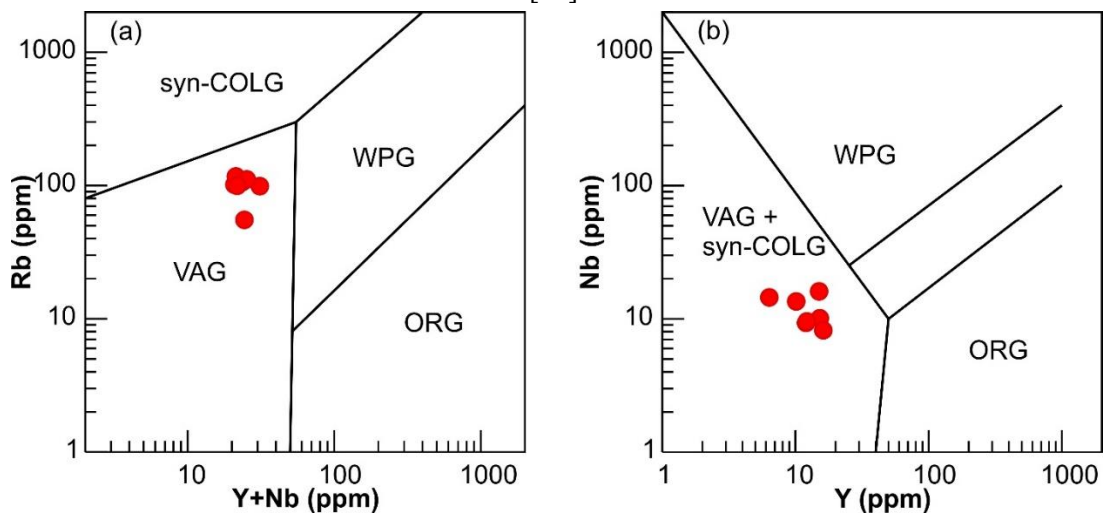


Fig. 5. Geotectonic classification of the Late Permian granitoid in Tra Phu-Tra Bong area based on trace element compositions [15]. VAG: volcanic arc granite, Syn-COLG: syn-collision granite, ORG: ocean ridge granite and WPG: within plate granite.

4.2. Zircon U-Pb geochronology

Tab. 2. Zircon U-Pb analytical data of the Tra Bong granite μm

Sample	Th/U	Isotopic ratios						Age (Ma)				Conc%
		$^{207}\text{Pb}/^{206}\text{Pb}$	1 σ	$^{207}\text{Pb}/^{235}\text{U}$	1 σ	$^{206}\text{Pb}/^{238}\text{U}$	1 σ	$^{206}\text{Pb}/^{238}\text{U}$	1 σ	$^{207}\text{Pb}/^{235}\text{U}$	1 σ	
TB27	15°15'07.2"N, 108°32'53.2"E											
-1	0.5 2	0.0545 9	0.0023 3	0.3065 5	0.0129 4	0.0407 3	0.0007 4	257	5	272	10	94
-2	0.8 3	0.0513 1	0.0017 7	0.2872 7	0.0099 1	0.0406 1	0.0006 5	257	4	256	8	100
-3	0.6 5	0.0512 8	0.0021 8	0.2865 9	0.0121 4	0.0405 4	0.0007 2	256	4	256	10	100
-4	0.6 4	0.0515 3	0.0018 0	0.2889 8	0.0101 5	0.0406 7	0.0006 6	257	4	258	8	100
-5	0.5 8	0.0514 2	0.0015 0	0.2785 8	0.0082 9	0.0393 0	0.0006 2	248	4	250	7	99
-6	0.4 1	0.0513 6	0.0018 4	0.2781 6	0.0100 0	0.0392 9	0.0006 6	248	4	249	8	100
-7	0.8 1	0.0516 7	0.0016 8	0.2892 8	0.0095 3	0.0406 1	0.0006 7	257	4	258	8	100
-8	0.5 5	0.0520 9	0.0025 9	0.2877 5	0.0140 4	0.0400 7	0.0007 5	253	5	257	11	98
-9	0.5 2	0.0517 6	0.0015 6	0.2850 9	0.0087 0	0.0399 5	0.0006 3	253	4	255	7	99
-10	0.6 1	0.0514 5	0.0020 4	0.2845 1	0.0112 1	0.0401 1	0.0006 9	254	4	254	9	100
-11	0.4 5	0.0512 8	0.0013 6	0.2838 9	0.0077 0	0.0401 6	0.0006 1	254	4	254	6	100
-12	0.5 5	0.0526 2	0.0020 4	0.2926 8	0.0112 3	0.0403 5	0.0006 8	255	4	261	9	98
-13	0.5 8	0.0616 8	0.0013 5	0.3470 7	0.0079 1	0.0408 2	0.0006 0	258	4	303	6	85
-14	0.6 0	0.0897 2	0.0030 7	0.4941 4	0.0168 5	0.0399 5	0.0007 3	253	5	408	11	62
-15	0.6 9	0.0516 7	0.0011 4	0.2979 9	0.0069 3	0.0418 4	0.0006 1	264	4	265	5	100
-16	0.7 6	0.0512 2	0.0008 7	0.2898 3	0.0055 3	0.0410 5	0.0005 9	259	4	258	4	100
-17	0.7 1	0.0513 6	0.0019 0	0.2810 2	0.0104 9	0.0396 9	0.0006 9	251	4	251	8	100
TB28	15°15'18.9"N, 108°33'20.9"E											
-1	0.6 6	0.0562 3	0.0008 3	0.5723 3	0.0091 8	0.0738 3	0.0009 3	459	6	460	6	100
-2	0.4 8	0.0515 2	0.0010 6	0.2825 8	0.0059 7	0.0397 8	0.0005 3	251	3	253	5	99
-3	0.4 1	0.0614 8	0.0018 5	0.3505 3	0.0104 9	0.0413 7	0.0006 3	261	4	305	8	86
-4	0.5	0.0512	0.0009	0.2774	0.0054	0.0392	0.0005	248	3	249	4	100

Sample	Th/U	Isotopic ratios						Age (Ma)				
		²⁰⁷ Pb/ ²⁰⁶ Pb	1σ	²⁰⁷ Pb/ ²³⁵ U	1σ	²⁰⁶ Pb/ ²³⁸ U	1σ	²⁰⁶ Pb/ ²³⁸ U	1σ	²⁰⁷ Pb/ ²³⁵ U	1σ	Conc%
	6	9	9	5	8	4	0					
-5	0.3	0.0556	0.0008	0.5309	0.0087	0.0692	0.0008	432	5	432	6	100
	1	3	7	2	4	3	6					
-6	0.5	0.0514	0.0022	0.2813	0.0123	0.0396	0.0007	251	4	252	10	100
	2	1	8	9	3	7	2					
-7	0.6	0.0513	0.0018	0.2823	0.0104	0.0398	0.0006	252	4	253	8	100
	0	7	9	8	2	5	6					
-8	0.4	0.0515	0.0019	0.2907	0.0109	0.0408	0.0007	258	4	259	9	100
	9	5	4	5	6	8	0					
-9	0.7	0.0515	0.0025	0.2883	0.0137	0.0405	0.0007	256	5	257	11	100
	4	1	0	1	9	8	8					
-10	0.4	0.0515	0.0020	0.2790	0.0111	0.0392	0.0006	248	4	250	9	99
	8	8	6	8	3	4	9					
-11	0.8	0.0514	0.0025	0.2853	0.0137	0.0402	0.0007	254	5	255	11	100
	4	0	0	3	3	6	9					
-12	0.5	0.0528	0.0025	0.2874	0.0138	0.0394	0.0007	249	5	257	11	97
	8	7	8	5	4	4	7					
-13	0.8	0.0517	0.0022	0.2885	0.0124	0.0404	0.0007	255	5	257	10	99
	1	5	4	4	3	2	5					
-14	0.7	0.0515	0.0020	0.2805	0.0109	0.0395	0.0006	250	4	251	9	100
	4	0	0	9	2	3	9					
-15	0.8	0.0512	0.0015	0.2763	0.0085	0.0391	0.0006	248	4	248	7	100
	5	3	6	4	9	4	2					
-16	0.4	0.0518	0.0018	0.2980	0.0108	0.0417	0.0007	264	4	265	8	100
	7	1	6	9	1	6	1					

$$\text{Conc.}\% = ((^{206}\text{Pb}/^{238}\text{U})/(^{207}\text{Pb}/^{235}\text{U})) * 100$$

The U-Pb zircon isotopic age analysis results for samples TB27 and TB28, comprising a total of 33 analysis points, are presented in Table 2.

Cathodoluminescence (CL) images of representative zircon species from samples TB27 and TB28 (Figure 6) indicate that zircon grains vary in size from 150 to 350 μm. Zircon from sample TB28 exhibits a short prism morphology, is euhedral, and displays typical oscillatory zoning typical of the magmatic zircon (Figure 6). In contrast, zircon grains from sample TB27 are subhedral and exhibit a patchy zoning texture. The images concentrate on the central region of zircon grains.

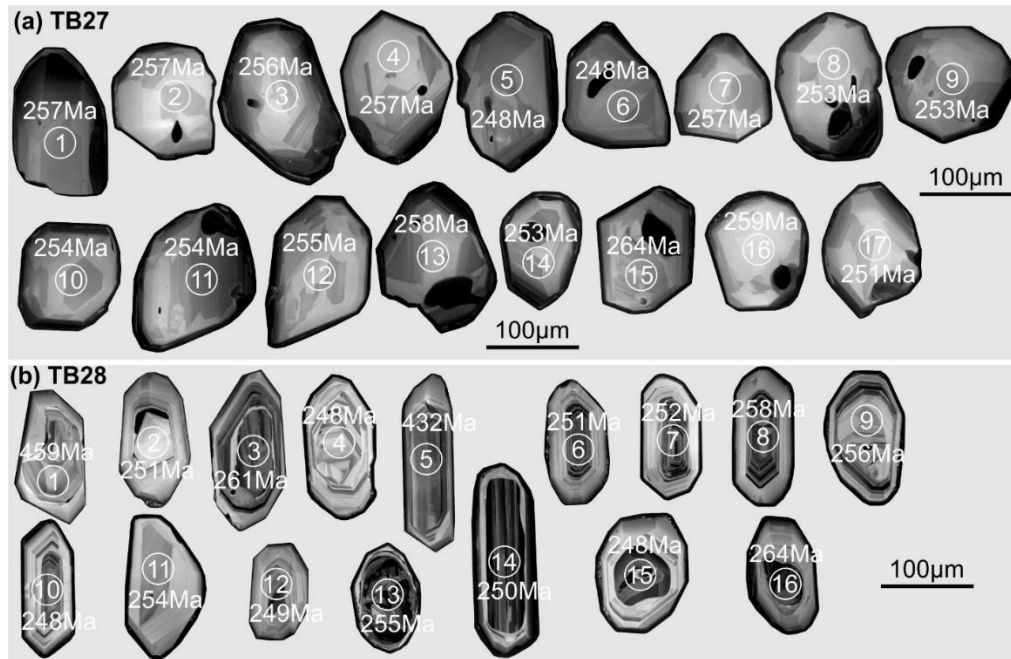


Fig. 6. Cathodoluminescence (CL) images of the Late Permian granitoid in Tra Phu-Tra Bong area. The circles represent the LA-ICP-MS U-Pb zircon analysis point, measuring 35 μ m in diameter

Sample TB27 (Coordinates: 15°15'07.2"N, 108°32'53.2"E): LA-ICP-MS U-Pb zircon age analysis of 17 points yielded $^{206}\text{Pb}/^{238}\text{U}$ age values between 248 Ma and 264 Ma, with an average of 255 ± 2.0 Ma (Figure 7a,b), indicating the crystallization age of the Late Permian granodiorite from sample TB27.

Sample TB28 (Coordinates: 15°15'18.9"N, 108°33'20.9"E): LA-ICP-MS U-Pb zircon age analysis of 16 points yielded $^{206}\text{Pb}/^{238}\text{U}$ age values between 248 Ma and 264 Ma, with a mean of 252 ± 2.2 Ma (Figure 7c,d). Two points showed ages of 432 Ma and 459 Ma, potentially representing inherited zircon ages (Figure 7e). Most age points yield values that align between 97% and 100%. Granodioritic sample TB28 exhibits a Late Permian crystallization age.

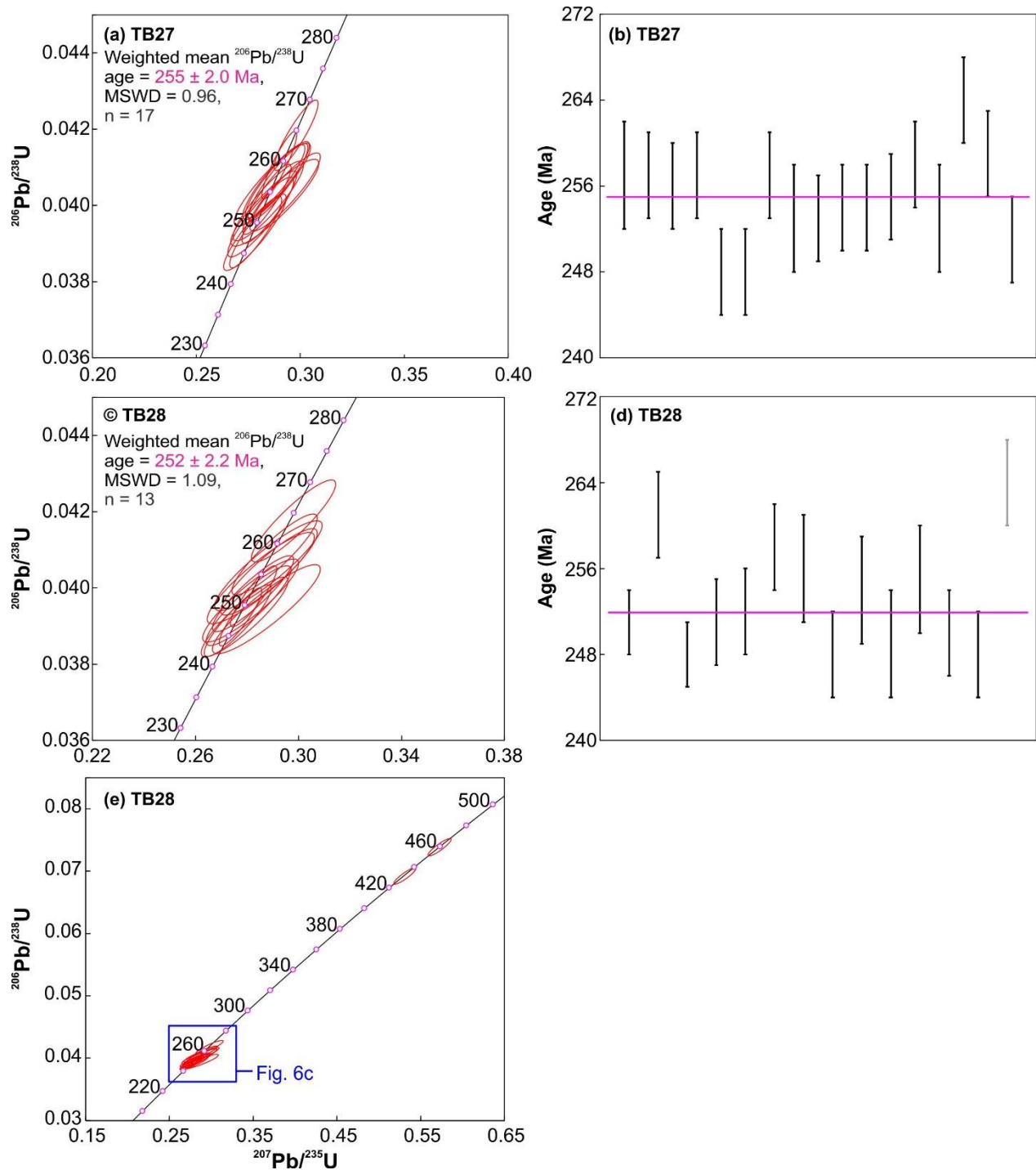


Fig. 7. a, b: The Concordia plot and the weighted mean diagrams for the LA-ICP-MS U-Pb zircon ages from the sample TB27; c, d: The Concordia plot and the average age for the LA-ICP-MS U-Pb zircon ages from the sample TB28.

5. Discussion

5.1. Emplacement age

The Tra Bong complex is comprised of the Tra Bong block and the southern part of the Tra My block (Figure 1b). The Tra Bong granite is observed to penetrate the Chu Lai granite and the Kham Duc metasedimentary formation, while it is unconformably overlain by Quaternary sediments. In the geological and mineral mapping of the Quang Ngai sheet at a scale of 1:200,000, Nguyen Van Trang (1986) categorized the Tra Bong block as Ordovician-Silurian in age, drawing conclusions from the consistent relationship observed

between the Tra Bong granitoids and metamorphic rocks. The isotopic age analysis results for the all rocks of the Tra Bong block indicate ages of 387 Ma and 443 Ma [20]. To date, there has been no investigation utilizing the U-Pb zircon technique to ascertain the age of the Tra Bong granitoids.

This study involved the analysis of U-Pb zircon isotopic ages from two samples, TB27 and TB28, encompassing a total of 33 analytical points. The U-Pb zircon isotopic method was employed to determine $^{206}\text{Pb}/^{238}\text{U}$ ages, which ranged from 255 Ma to 252 Ma. These ages are considered to be the crystallization ages of the Tra Bong granitoid in the Late Permian period. This firstly represents U-Pb zircon isotopic age results obtained through the LA-ICP-MS method, indicating that these formations (Late Permian age) are much younger than previous studies.

5.2. Petrogenesis of Tra Phu-Tra Bong granitoid and its tectonic implications

According to the classification system for I-, S-, and A-type granites, the Tra Bong granite in the study area exhibits numerous characteristics of I-type granite. In the field, Tra Bong granites lack metasedimentary xenoliths from the previous formations. The classification system of granitoids [21] indicates that the mineral assemblages of Tra Bong granite are abundant in hydrous-rich minerals such as hornblende and biotite, while impoverished in aluminum-rich minerals like muscovite and cordierite (Figure 3), corresponding to I-type granite.

In terms of geochemical characteristics (Table 1), Tra Bong granite is classified within the calc-alkaline series, exhibiting medium to high alkaline content and categorized as Na-K alkaline. The examination of the primary components reveals that these granites are categorized as I-type granite, which is in complete agreement with the results obtained from the mineral assemblage analysis performed with a polarizing microscopy. The presence of hornblende, biotite, and especially sphene minerals serves as indicators of the I-type granite Permian-Triassic stage in the study area. Previous investigations by domestic and international geologists revealed that the Indochina area was formed from various continental and microcontinental plates such as Indochina, South China, Sibumasu, and Simao that broke from the Gondwana continent [3, 6-8, 22]. During the late Permian to early Triassic periods, several microplates merged to create the present-day Indochina plate [6, 7, 11]. Within the territory of Vietnam, the collision boundaries between them are mainly manifested in the Kontum massif, the Truong Son belt, and the Song Ma suture (Figure 8).

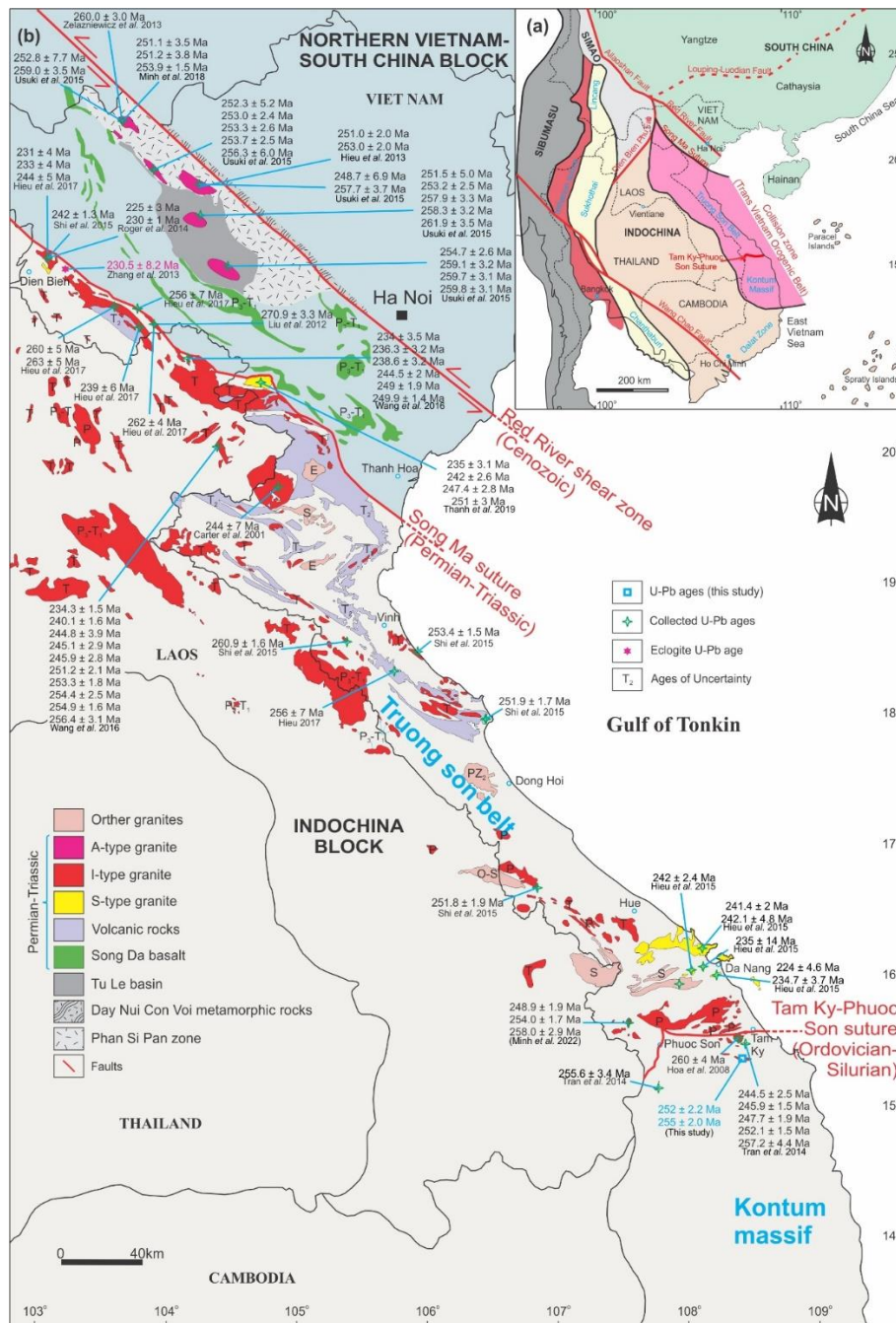


Fig. 8. (a) Tectonic map of central and eastern Asia and (b) Simplified geological map of the Indochina block indicating emplacement times of Permian-Triassic formations [7, 9]

Vietnam's Late Permian-Early Triassic magmatic activity is widely dispersed throughout the Song Ma suture, the Truong Son belt, and the Kontum massif. Their formation process is thought to be related to the convergence between the Indochina and Indochina plates during the Permian-Triassic period [4-7, 9-11, 23, 24] (Table 3, Figure 8). The granitoids from this period consist of three types of granite: A-, I-, and S-type granite. Among these, I- and S-type granites are the most prevalent and are extensively found in the Song Ma suture, Truong Son orogenic belt, and Kontum massif. This study identifies the Tra Phu-Tra Bong plutonic granitoid as I-type granites, formed between 255–252 Ma, corresponding to the late Palaeozoic period. The spatial distribution around the Kontum massif and Truong Son orogenic belt indicates that the Tra Phu-Tra Bong granites are associated with magmatic complexes from the same Permian-Triassic period. They are comparable to the Ben Giang-Que Son complexes, which show an age of 278–285 Ma [11], and the Cha Val granitoids with an age of 249–258 Ma [9] in terms of composition and formation age.

Tab. 3. Ages of Permi-Triassic plutonic and volcanic rocks in Viet Nam.

Sample	Rock type	Age (Ma)	Method	Material	Reference
TB27	Granite	255 ± 2.0	LA-ICP-MS	zircon	This study
TB28	Granite	252 ± 2.2	LA-ICP-MS	zircon	This study
KTM-GbDi1918	Diorite	248.9 ± 1.9	LA-ICP-MS	zircon	Minh <i>et al.</i> 2022
KTM-GbDi1921	Diorite	258.0 ± 2.9	LA-ICP-MS	zircon	Minh <i>et al.</i> 2022
KTM-Di1922	Diorite	254.0 ± 1.7	LA-ICP-MS	zircon	Minh <i>et al.</i> 2022
S1	Gneiss	243 ± 7	LA-ICP-MS	zircon	Nakano <i>et al.</i> 2021
S2	Gneiss	236 ± 8 Ma	LA-ICP-MS	zircon	Nakano <i>et al.</i> 2021
i1	Gneiss	238 ± 4 Ma	LA-ICP-MS	zircon	Nakano <i>et al.</i> 2021
i2	Gneiss	232 ± 9 Ma	LA-ICP-MS	zircon	Nakano <i>et al.</i> 2021
i3	Gneiss	238 ± 6 Ma	LA-ICP-MS	zircon	Nakano <i>et al.</i> 2021
i4	Gneiss	238 ± 8 Ma	LA-ICP-MS	zircon	Nakano <i>et al.</i> 2021
i5	Gneiss	238 ± 5 Ma	LA-ICP-MS	zircon	Nakano <i>et al.</i> 2021
i6	Gneiss	238 ± 5 Ma	LA-ICP-MS	zircon	Nakano <i>et al.</i> 2021
i7	Granulite	238 ± 5 Ma	LA-ICP-MS	zircon	Nakano <i>et al.</i> 2021
i8	Granulite	243 ± 7 Ma	LA-ICP-MS	zircon	Nakano <i>et al.</i> 2021
GO09	Gabbro	250.1 ± 1.5	LA-ICP-MS	zircon	Tran <i>et al.</i> 2020
MLT42	Monzogranite	235 ± 3.1	LA-ICP-MS	zircon	Thanh <i>et al.</i> 2019
MLT34	Monzogranite	242 ± 2.6	LA-ICP-MS	zircon	Thanh <i>et al.</i> 2019
MLT09	Granodiorite	247.4 ± 2.8	LA-ICP-MS	zircon	Thanh <i>et al.</i> 2019
MLT08	Monzogranite	251 ± 3	LA-ICP-MS	zircon	Thanh <i>et al.</i> 2019
V0927	Granite	251.1 ± 3.5	LA-ICP-MS	zircon	Minh <i>et al.</i> 2018
V0926	Granite	251.2 ± 3.8	LA-ICP-MS	zircon	Minh <i>et al.</i> 2018
V0928	Granite	253.9 ± 1.5	LA-ICP-MS	zircon	Minh <i>et al.</i> 2018
V0905	Granodiorite	231 ± 4	LA-ICP-MS	zircon	Hieu <i>et al.</i> 2017
V0903	Granodiorite	233 ± 4	LA-ICP-MS	zircon	Hieu <i>et al.</i> 2017

V1106	Granite	239 ± 6	LA-ICP-MS	zircon	Hieu <i>et al.</i> 2017
V0908	Biotite granite	244 ± 5	LA-ICP-MS	zircon	Hieu <i>et al.</i> 2017
V0821	Tonalite	256 ± 7	LA-ICP-MS	zircon	Hieu <i>et al.</i> 2017
V0741	Granite	260 ± 5	LA-ICP-MS	zircon	Hieu <i>et al.</i> 2017
V0738	Quartz diorite	262 ± 4	LA-ICP-MS	zircon	Hieu <i>et al.</i> 2017
V0856	Granite	263 ± 5	LA-ICP-MS	zircon	Hieu <i>et al.</i> 2017
R11	Rhyolite	256 ± 7	LA-ICP-MS	zircon	Hieu 2017
LH16	Tonalite	234 ± 3.5	LA-ICP-MS	zircon	Wang <i>et al.</i> 2016
LC16	Monzogranite	234.3 ± 1.5	LA-ICP-MS	zircon	Wang <i>et al.</i> 2016
LH13	Tonalite	236.3 ± 3.2	LA-ICP-MS	zircon	Wang <i>et al.</i> 2016
LH11	Tonalite	238.6 ± 3.2	LA-ICP-MS	zircon	Wang <i>et al.</i> 2016
LT4	Granodiorite	240.1 ± 1.6	LA-ICP-MS	zircon	Wang <i>et al.</i> 2016
LH4	Granodiorite	244.5 ± 2	LA-ICP-MS	zircon	Wang <i>et al.</i> 2016
LT6	Granodiorite	244.8 ± 3.9	LA-ICP-MS	zircon	Wang <i>et al.</i> 2016
LC1	Monzogranite	245.1 ± 2.9	LA-ICP-MS	zircon	Wang <i>et al.</i> 2016
LC8	Monzogranite	245.9 ± 2.8	LA-ICP-MS	zircon	Wang <i>et al.</i> 2016
LH1	Granodiorite	249 ± 1.9	LA-ICP-MS	zircon	Wang <i>et al.</i> 2016
LH5	Granodiorite	249.9 ± 1.8	LA-ICP-MS	zircon	Wang <i>et al.</i> 2016
LC17	Monzogranite	251.2 ± 2.1	LA-ICP-MS	zircon	Wang <i>et al.</i> 2016
LC12	Monzogranite	253.3 ± 1.8	LA-ICP-MS	zircon	Wang <i>et al.</i> 2016
LT1	Granodiorite	254.4 ± 2.5	LA-ICP-MS	zircon	Wang <i>et al.</i> 2016
LC6	Monzogranite	254.9 ± 1.6	LA-ICP-MS	zircon	Wang <i>et al.</i> 2016
LT3	Granodiorite	256.4 ± 3.1	LA-ICP-MS	zircon	Wang <i>et al.</i> 2016
V1102-3	Granite	224 ± 4.6	LA-ICP-MS	zircon	Hieu <i>et al.</i> 2015
V1102	Granite	234.7 ± 3.7	LA-ICP-MS	zircon	Hieu <i>et al.</i> 2015
V1124	Granite	235 ± 14	LA-ICP-MS	zircon	Hieu <i>et al.</i> 2015
V1127	Granite	241.4 ± 2	LA-ICP-MS	zircon	Hieu <i>et al.</i> 2015

V1125	Granite	242.1 ± 4.8	MS LA-ICP-MS	zircon	Hieu <i>et al.</i> 2015
V1114	Granite	242 ± 2.4	MS LA-ICP-MS	zircon	Hieu <i>et al.</i> 2015
VN12-066	Granodiorites	242.2 ± 1.3	MS LA-ICP-MS	zircon	Shi <i>et al.</i> 2015
VN12-050	Plagiogranite	251.8 ± 1.9	MS LA-ICP-MS	zircon	Shi <i>et al.</i> 2015
VN12-025	Rhyolite	251.9 ± 1.7	MS LA-ICP-MS	zircon	Shi <i>et al.</i> 2015
VN12-022	Monzogranite	253.4 ± 1.5	MS LA-ICP-MS	zircon	Shi <i>et al.</i> 2015
VN12-056	Monzogranites	260.9 ± 1.6	MS LA-ICP-MS	zircon	Shi <i>et al.</i> 2015
LTH26A	Granite	248.7 ± 6.9	MS LA-ICP-MS	zircon	Usuki <i>et al.</i> 2015
LB19A	Ryholite	251.5 ± 5.0	MS LA-ICP-MS	zircon	Usuki <i>et al.</i> 2015
YB27	Granite	252.3 ± 5.2	MS LA-ICP-MS	zircon	Usuki <i>et al.</i> 2015
LTH9	Granite	252.8 ± 7.7	MS LA-ICP-MS	zircon	Usuki <i>et al.</i> 2015
YB24	Granite	253.0 ± 2.4	MS LA-ICP-MS	zircon	Usuki <i>et al.</i> 2015
YB21	Ryholite	253.2 ± 2.5	MS LA-ICP-MS	zircon	Usuki <i>et al.</i> 2015
BK6	Granite	253.3 ± 2.6	MS LA-ICP-MS	zircon	Usuki <i>et al.</i> 2015
YB29	Granite	253.7 ± 2.5	MS LA-ICP-MS	zircon	Usuki <i>et al.</i> 2015
YB12	Ryholite	254.6 ± 2.6	MS LA-ICP-MS	zircon	Usuki <i>et al.</i> 2015
PSP37	Granite	256.3 ± 6.0	MS LA-ICP-MS	zircon	Usuki <i>et al.</i> 2015
LTH21A	Granite	257.7 ± 3.7	MS LA-ICP-MS	zircon	Usuki <i>et al.</i> 2015
LTH81-3	Ryholite	257.9 ± 3.3	MS LA-ICP-MS	zircon	Usuki <i>et al.</i> 2015
LTH82	Ryholite	258.3 ± 3.2	MS LA-ICP-MS	zircon	Usuki <i>et al.</i> 2015
LTH12	Granite	259.0 ± 3.5	MS LA-ICP-MS	zircon	Usuki <i>et al.</i> 2015
LTH77	Ryholite	259.1 ± 3.2	MS LA-ICP-MS	zircon	Usuki <i>et al.</i> 2015
LTH76A	Ryholite	259.7 ± 3.1	MS LA-ICP-MS	zircon	Usuki <i>et al.</i> 2015
LTH76B	Ryholite	259.8 ± 3.1	MS LA-ICP-MS	zircon	Usuki <i>et al.</i> 2015
LTH81-1	Ryholite	261.9 ± 3.5	MS LA-ICP-MS	zircon	Usuki <i>et al.</i> 2015
JH0804	Granitic gneiss	244.5 ± 2.5	MS LA-ICP-MS	zircon	Tran <i>et al.</i> 2014

JH0822	Granite	245.9 ± 1.5	LA-ICP-MS	zircon	Tran <i>et al.</i> 2014
HRDD221	Paragneiss	247.7 ± 1.9	LA-ICP-MS	zircon	Tran <i>et al.</i> 2014
JH0810	Granodiorite	252.1 ± 1.5	LA-ICP-MS	zircon	Tran <i>et al.</i> 2014
KD10-32/1	Diorite	255.6 ± 3.4	LA-ICP-MS	zircon	Tran <i>et al.</i> 2014
DCL09	Dioritic gneiss	257.2 ± 4.4	LA-ICP-MS	zircon	Tran <i>et al.</i> 2014
VT 225	Granite	225 ± 3	LA-ICP-MS	zircon	Roger <i>et al.</i> 2014
VT 226	Granite	230 ± 1	LA-ICP-MS	zircon	Roger <i>et al.</i> 2014
V0783	Granite	251.0 ± 2.0	LA-ICP-MS	zircon	Hieu <i>et al.</i> 2013
V0779	Granite	253.0 ± 2.0	LA-ICP-MS	zircon	Hieu <i>et al.</i> 2013
V0789	Granite	251.0 ± 2.0	LA-ICP-MS	zircon	Hieu <i>et al.</i> 2013
V0786	Granite	253.0 ± 2.0	LA-ICP-MS	zircon	Hieu <i>et al.</i> 2013
MH	Granite	260.0 ± 3.0	SHRIMP	zircon	Anczkiewicz <i>et al.</i> 2013
11SM5I	Eclogite	230.5 ± 8.2	SHRIMP	zircon	Zhang <i>et al.</i> 2013
V0829	Quartz diorite	270.9 ± 3.3	LA-ICP-MS	zircon	Liu <i>et al.</i> 2012
	Granite	260 ± 4	SHRIMP	zircon	Hoa <i>et al.</i> 2008
VN 09	Gneiss	244 ± 7	SHRIMP	zircon	Carter <i>et al.</i> 2001

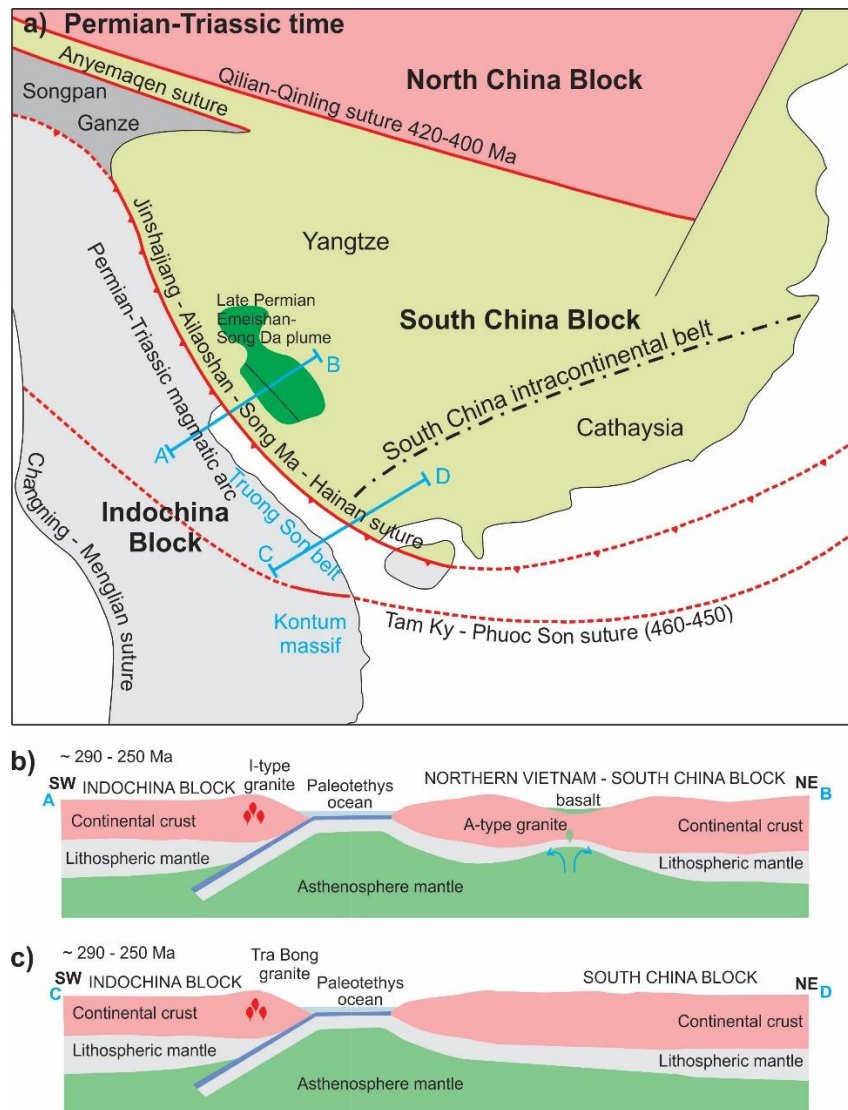


Fig. 9. Schematic model for magma evolution during the Indochina block and its adjacent areas in the Permian-Triassic [9, 25]

Barbarin (1999) proposed the origin and mechanism of magmatic activity of metaluminous I-type granite, classifying granitoids based on the Wilson cycle to associate them with two main tectonic contexts: (1) magmatic activity related to the Andean-type continental arc and (2) post-orogenic lithospheric extension. This study identifies the Tra Phu-Tra Bong plutonic granitoids as metaluminous I-type granite, associated with subduction magmatic activity (Figure 5a,b). It is posited that these granitoids formed during the subduction phase (290–250 Ma) of the Paleo-Tethys ocean beneath the Indochina block along the Song Ma suture zone (Figure 9).

6. Conclusions

The granitic formations in the Tra Phu and Tra Bong areas predominantly consist of granodiorite and biotite granite. In the field, they crosscut the Chu Lai granite and the metasedimentary rocks of the Kham Duc formation and are unconformably overlain by Quaternary sediments. The mineral composition includes plagioclase, orthoclase, quartz, and feric minerals such as hornblende and biotite, in addition to sphene, typical of I-type granite.

The crystallization age of granitoids in the Tra Phu and Tra Bong areas was established using the LA-ICP-MS U-Pb zircon method, yielding ages of 255-252 Ma, indicative of the Late Permian period. This age is significantly younger than findings from prior studies, which suggested an Ordovician to Silurian age. The

granitoid formation in the Tra Phu and Tra Bong areas is likely associated with the convergence of the Indochina and South China blocks during the Late Permian to Early Triassic.

Acknowledgments

This research is funded by Vietnam National University, Ho Chi Minh City (VNU-HCM) under grant number C2022-18-29. Authors thank the anonymous reviewers for improving the manuscript.

Literature - References

1. Thuc D.D., Trung H., 1995. Vietnam geology, part of II: magma. ed. Hanoi: Department of Geology and Mineral Resources Survey, Science and Technics Publishing House. 359.
2. Lepvrier C., Van Vuong N., Maluski H., Truong Thi P., Van Vu T., 2008. Indosinian tectonics in Vietnam. *Comptes Rendus Geoscience*, 340(2-3), 94-111.
3. Faure M., Lepvrier C., Nguyen V.V., Vu T.V., Lin W., Chen Z., 2014. The South China block-Indochina collision: Where, when, and how? *Journal of Asian Earth Sciences*, 79, 260-274.
4. Hieu P.T., Yang Y.-Z., Binh D.Q., Nguyen T.B.T., Dung L.T., Chen F., 2015. Late Permian to Early Triassic crustal evolution of the Kontum massif, central Vietnam: zircon U–Pb ages and geochemical and Nd–Hf isotopic composition of the Hai Van granitoid complex. *International Geology Review*, 57(15), 1877-1888.
5. Shi M.-F., Lin F.-C., Fan W.-Y., Deng Q., Cong F., Tran M.-D., Zhu H.-P., Wang H., 2015. Zircon U–Pb ages and geochemistry of granitoids in the Truong Son terrane, Vietnam: Tectonic and metallogenic implications. *Journal of Asian Earth Sciences*, 101, 101-120.
6. Hieu P.T., Li S.-Q., Yu Y., Thanh N.X., Dung L.T., Tu V.L., Siebel W., Chen F., 2017. Stages of late Paleozoic to early Mesozoic magmatism in the Song Ma belt, NW Vietnam: evidence from zircon U–Pb geochronology and Hf isotope composition. *International Journal of Earth Sciences*, 106(3), 855-874.
7. Thanh T.V., Hieu P.T., Minh P., Nhuan D.V., Thuy N.T.B., 2019. Late Permian-Triassic granitic rocks of Vietnam: the Muong Lat example. *International Geology Review*, 61(15), 1823-1841.
8. Qian X., Wang Y., Zhang Y., Zhang Y., Senebottalath V., Zhang A., He H., 2019. Petrogenesis of Permian–Triassic felsic igneous rocks along the Truong Son zone in northern Laos and their Paleotethyan assembly. *Lithos*, 328-329, 101-114.
9. Minh P., Trung H.P., Kawaguchi K., Quynh A.N.T., Le Duc P., 2022. Geochemistry, zircon U–Pb geochronology and Sr–Nd–Hf isotopic composition of the Cha Val plutonic rocks in central Vietnam: Implications for Permian-Triassic Paleo-Tethys subduction-related magmatism. *Vietnam Journal of Earth Sciences*, 44(3), 301-326.
10. Dung N.T., Anh T.T., Hieu P.T., Minh P., Truong L.X., Minh N.T., Hung D.D., 2024. Crustal evolution of Paleozoic-Mesozoic granitoid in Dakrong-A Luoi area, Truong Son belt, central Vietnam: evidence from zircon U–Pb geochronology, geochemistry, and Hf isotope composition. *International Geology Review*, 1-25.
11. Thuy N.T.B., Hieu P.T., Xin Q., Xuan N.T., Minh P., Thu H.T., 2024. Zircon U–Pb Geochronology, Geochemistry, and Sr–Nd–Hf Isotopic Composition of Ben Giang-Que Son Complex in the Southern Truong Son Belt: Implications for Permian–Triassic Tectonic Evolution. *Minerals*, 14(6), 569.
12. Tran H.T., Zaw K., Halpin J.A., Manaka T., Meffre S., Lai C.-K., Lee Y., Le H.V., Dinh S., 2014. The Tam Ky-Phuoc Son Shear Zone in central Vietnam: Tectonic and metallogenic implications. *Gondwana Research*, 26(1), 144-164.
13. Nguyen Q.M., Feng Q., Zi J.-W., Zhao T., Tran H.T., Ngo T.X., Tran D.M., Nguyen H.Q., 2019. Cambrian intra–oceanic arc trondhjemite and tonalite in the Tam Ky–Phuoc Son Suture Zone, central Vietnam: Implications for the early Paleozoic assembly of the Indochina Block. *Gondwana Research*, 70, 151-170.
14. Wilson M., 1989. *Igneous petrogenesis*. Unwin Hyman. ed.: London.
15. Pearce J.A., Harris N.B., Tindle A.G., 1984. Trace element discrimination diagrams for the tectonic interpretation of granitic rocks. *Journal of petrology*, 25(4), 956-983.
16. Maniar P.D., Piccoli P.M., 1989. Tectonic discrimination of granitoids. *Geological society of America bulletin*, 101(5), 635-643.
17. Peccerillo A., Taylor S., 1976. Geochemistry of eocene calc-alkaline volcanic rocks from the Kastamonu area, Northern Turkey. *Contributions to Mineralogy and Petrology*, 58, 63–81.
18. Barker F., *Trondhjemite: definition, environment and hypotheses of origin*, in *Developments in petrology*. 1979, Elsevier. p. 1-12.

19. Irvine T.N., Baragar W., 1971. A guide to the chemical classification of the common volcanic rocks. *Canadian journal of earth sciences*, 8(5), 523-548.
20. Bao N.X., Trung H., 1980. The distribution of intrusive magma formations, southern Vietnam (in Vietnamese). *Journal of Geology, Hanoi*, 41, 35-59.
21. Barbarin B., 1999. A review of the relationships between granitoid types, their origins and their geodynamic environments. *Lithos*, 46(3), 605-626.
22. Tri T.V., Khuc V., 2011. *Geology and earth resources of Vietnam*. ed. Ha Noi, Vietnam: Publishing House for Science and Technology. 634.
23. Hoa T.T., Anh T.T., Phuong N.T., Dung P.T., Anh T.V., Izokh A.E., Borisenko A.S., Lan C.Y., Chung S.L., Lo C.H., 2008. Permo-Triassic intermediate–felsic magmatism of the Truong Son belt, eastern margin of Indochina. *Comptes Rendus Geoscience*, 340(2-3), 112-126.
24. Hieu P.T., Anh N.T.Q., Minh P., Thuy N.T.B., 2020. Geochemistry, zircon U–PB ages and HF isotopes of the Muong Luan granitoid pluton, Northwest Vietnam and its petrogenetic significance. *Island Arc*, 29(1), e12330.
25. Faure M., Nguyen V.V., Hoai L.T.T., Lepvrier C., 2018. Early Paleozoic or Early-Middle Triassic collision between the South China and Indochina Blocks: The controversy resolved? Structural insights from the Kon Tum massif (Central Vietnam). *Journal of Asian Earth Sciences*, 166, 162-180.